2012 IEEE 7th International Power Electronics and Motion Control Conference - ECCE Asia
June 2-5, 2012, Harbin, China

A Novel 400Hz Shunt Active Power Filter for Aircraft Electrical Power System

Zhong Chen, Miao Chen
Jiangsu Key Laboratory of New Energy Generation and Power Conversion
Nanjing University of Aeronautics and Astronautics
Nanjing, P. R. China
chenz@nuaa.edu.cn

Abstract—**In order to fulfill the high reliability of the aeronautical application, a novel three-phase four-wire shunt active power filter is proposed in this paper. In this proposed configuration, traditional bridge which is composed of two power switches is replaced by the novel bridge composed of one power switch and one diode. The annoying "shoot-through" phenomenon is eliminated by using this novel configuration. Meanwhile, better efficiency and better performance brought by this novel configuration benefit the improvement of the compensation performance. Moreover, operation principle of the APF is analyzed in detail; current control strategy and the voltage balance control strategy for the split-capacitor topology are studied as well. Finally, a prototype with the compensating capacity of 3 kVA is designed. Simulation and experimental results are shown to confirm the validity and feasibility of the novel aeronautical active power filter.**

Keywords-shunt active power filter; aircraft power system; topology; control strategy

I. INTRODUCTION

The increasing use of electrical power in place of hydraulic, pneumatic, and mechanical power is the development tendency of the advanced and modern aircraft power systems [1][2]. However, the much more complicated fabrication of the electrical power system and large number of the avionics and power converters degrade the power quality and reliability of the system. The traditional harmonic compensation method including passive filter, multi-pulse rectifier, and active power factor correction could not fulfill the demand and requirement of the modern aircraft [3][4].

Being a highly advanced power quality regulation technology, active power filter has the best feasibility and widest prospect for its insensitive for the variation of system impedance and frequency and high dynamic response [5][6]. However, most researches about this topic usually focus on 50Hz application. With the development of the concept of the "all electric aircraft" and the "more electric aircraft" (MEA), more and more researchers start to study the APF applied in the aircraft electrical power system (EPS), to resolve the power quality issues [7]-[13]. In [8], a system model of variable-frequency variable-speed EPS of 90 kVA is built. Large numbers of simulation waveforms given in this paper confirm the feasibility of the APF, the harmonic current, reactive power, and unbalanced problem all getting resolved. In [9], a cascaded inverter based shunt APF is applied in the aeronautical AC EPS, and a novel predictive current control algorithm with high bandwidth is proposed. Simulation results confirm the good current tracking performance of the fabrication. In [10], an improved harmonic current detection algorithm based on the discreet FFT technology is proposed. Fundamental and harmonic components of 400Hz system could be estimated in a high speed. In [11], a multi-resolution based DSP control strategy is applied in the aeronautical APF, to reduce the calculation time and increase the detection accuracy and speed. Moreover, one-cycle control and space vector control have been used in the aeronautical APF in [12]. Generally speaking, most researches on the aeronautical APF application focus on the harmonic detection algorithm and current control strategy, few papers have discussed the topology of aeronautical APF. Most of the above active power filters are based on the three-phase three-leg shunt inverter, not matching the aeronautical four wires application.

In this paper, a novel aeronautical APF with high reliability is proposed. The annoying "shoot-through" phenomenon is eliminated by using this configuration composed of one power switch and one diode. Operation principle, current control method and voltage control strategy for the spit-capacitor based topology are studied as well. In order to verify the feasibility of the novel APF, a 3 kVA hardware prototype is built and tested in the laboratory.

II. NOVEL SHUNT ACTIVE POWER FILTER

A. Topology and Operation Principle

Fig. 1 illustrates the topology of novel aeronautical active power filter, which is based on a novel three-phase four-wire "spit-capacitor" configuration. Here, the middle point of dc capacitors C_1 and C_2 connects with the neutral point. The whole system consists of two parts: part I and part II, and each part are combined of a novel phase leg and a boost inductor. It should be noted that, the difference between these two parts is the opposite location of the diode and power switch in its leg.

The phase voltages u_S, load currents i_L, and the dc-link voltages U_1 and U_2 are detected and fed to the APF controller. After the APF controller's calculation, the compensation currents' reference for part I i_{C1}^*, i_{C3}^*, i_{C5}^* and part II i_{C2}^*, i_{C4}^*,

978-1-4577-2088-8/11/$26.00 ©2012 IEEE

i_{C6}^* will be obtained. The practical compensation current and the current reference will be sent into the current controller to derive the PWM drive signals of the novel APF.

As Fig. 1 illustrates, the practical compensation currents in part I i_{C1}, i_{C3}, i_{C5} flow into the aeronautical power system; and practical compensation current in part II i_{C2}, i_{C4}, i_{C6} flow out of the aeronautical power system. These two parts operate in the dual mode, sharing the whole practical compensation currents.

Before analyzing the operation principle of the novel APF, following assumptions are taken:

1) All of the inductances are equal L_1=L_2…=L_6=L, parasitic parameters are neglected;

2) Both of the dc capacitances are equal C_1=C_2=C, and the dc-link voltages are equal U_1=U_2=U_{dc};

3) Power switches S_1~S_6 and power diodes D_1~D_6 are all ideal;

According to the KCL, the relationship between the compensation currents i_C, the source currents i_S and load currents i_L could be expressed as follows:

$$\begin{cases} i_{Sa} - i_{La} - i_{Ca} = 0 \\ i_{Sb} - i_{Lb} - i_{Cb} = 0 \\ i_{Sc} - i_{Lc} - i_{Cc} = 0 \end{cases} \tag{1}$$

Here, $\begin{cases} i_{Ca} = -i_{C1} + i_{C2} \\ i_{Cb} = -i_{C3} + i_{C4} \\ i_{Cc} = -i_{C5} + i_{C6} \end{cases}$

When compensation currents flow through part I, part II stop working, and vice versa. Here, take the APF's operation of phase-*a* for example. Detailed operation stages are given in Fig. 2. Four different operation stages exist, according to the compensation current's direction.

When part II stops working, i_{C2}=0, power switch S_2 and D_2 are blocked, and power switch S_1 and D_1 in part I operate in high frequency to draw the needed compensation current.

1) Stage one, power switch S_1 conducts and diode D_1 switches off, when $i_{C1} \le i_{C1}^*$. The equivalent circuit is given in Fig. 2(a). Aeronautical APF regenerates the power to the power grid. Relationship between the compensation current i_{C1}, the phase voltage u_{Sa} and the dc-link voltage U_{dc} could be expressed as follows:

$$U_{dc} - u_{Sa} = L\frac{di_{C1}}{dt} \tag{2}$$

In this stage, compensation current i_{C1} increases at the rate of (U_{dc}-u_{Sa})/L, voltage stress of D_1 is 2U_{dc}.

2) Stage two, power switch S_1 switches off and diode D_1 conducts, when $i_{C1} > i_{C1}^*$. The equivalent circuit is given in Fig. 2(b). Aeronautical APF is supplied by the power grid. The relationship between the compensation current i_{C1}, the phase voltage u_{Sa} and the dc-link voltage U_{dc} could be expressed as follows:

$$-U_{dc} - u_{Sa} = L\frac{di_{C1}}{dt} \tag{3}$$

In this stage, compensation current i_{C1} decreases at the rate of (U_{dc}+u_{Sa})/L, voltage stress of S_1 is 2U_{dc}.

When part I stops working, i_{C1}=0, power switch S_1 and D_1 are blocked, and power switch S_2 and D_2 in part II operate in high frequency to draw the needed compensation current.

3) Stage three, diode D_2 switches off and power switch S_2 conducts, when $i_{C2} \le i_{C2}^*$. The equivalent circuit is given in Fig. 2(c). Aeronautical APF regenerates the power to the power grid. Relationship between the compensation current i_{C2}, the phase voltage u_{Sa} and the dc-link voltage U_{dc} could be expresses as follows:

$$U_{dc} + u_{Sa} = L\frac{di_{C2}}{dt} \tag{4}$$

In this stage, compensation current i_{C2} increases at the rate of (U_{dc}+u_{Sa})/L, voltage stress of D_2 is 2U_{dc}.

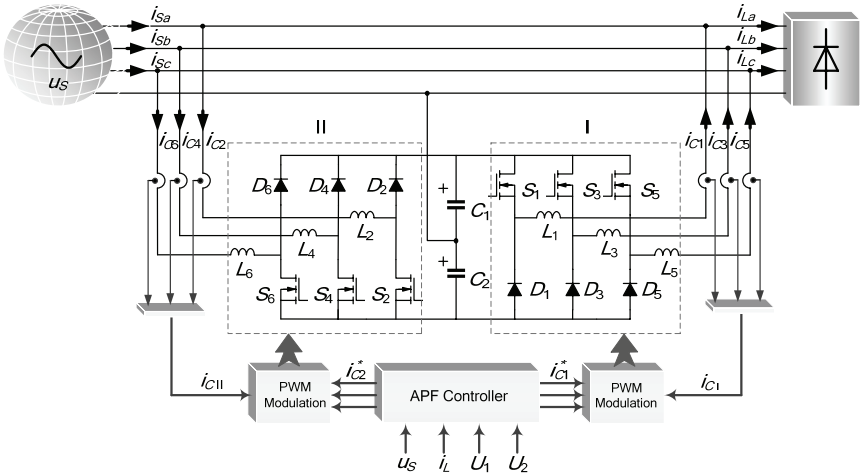

Figure 1. System diagram of the proposed aeronautical active power filter

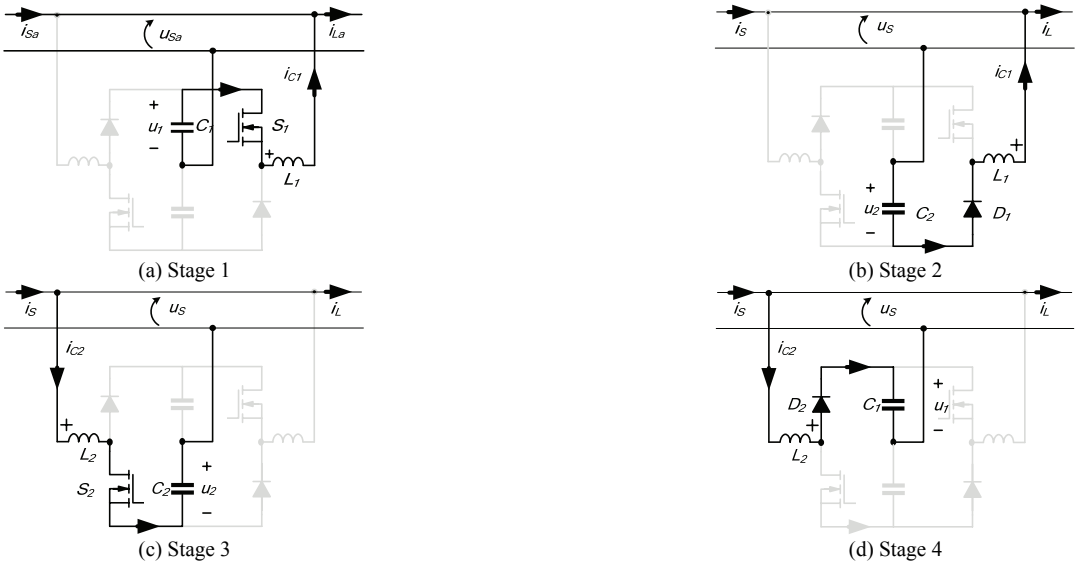

Figure 2. Equivalent circuit of each operation stage

4) Stage four, diode D_2 conducts and power switch S_2 switches off, when $i_{C2}>i_{C2}^*$. The equivalent circuit is given in Fig. 2(d). Aeronautical APF is supplied by the power grid. The relationship between the compensation current i_{C2}, the phase voltage u_S and the dc-link voltage U_{dc} could be expressed as follows:

$$-U_{dc}+u_{Sa}=L\frac{di_{C2}}{dt} \tag{5}$$

In this stage, compensation current i_{C2} decreases at the rate of $(U_{dc}\text{-}u_{Sa})/L$, voltage stress of S_2 is $2U_{dc}$.

B. Characteristic Analysis

In the traditional leg combined of two power switches based DC/AC converter, AC/DC converter and APF, a dead-time is required to be added into the PWM signals to avoid the "shoot-through" phenomenon. However, in the practical application, the increasing of switching frequency contradicts the power capacity's increasing. Usually, in the large power application, power converter operates at a low frequency. In the aeronautic electrical power system with the requirement of high reliability, the dead-time needs increased to be larger, and the frequency needs decreased to be smaller. Therefore, the compensation performance will be deteriorated in the limit switching frequency and larger dead-time.

In the novel APF, traditional leg is replaced by the single switch based bridge leg, in which the "shoot through" is eliminated inherently. Furthermore, the selection of power switches and diodes gets decoupled in the novel configuration. The diodes with higher performance could be used to achieve better free-wheel performance and smaller loss instead of the body-diode. Consequently, no "dead-time" behavior brought by this configuration increases the compensation accuracy and decreases the compensation errors. Meanwhile, switching frequency of the novel APF could be increased for further.

III. Control Strategy of Compensation Current and DC-Link Voltage

In the novel APF, two similar parts of power converters work corporately. In order to ensure APF's operation with high efficiency and high reliability, special and original control strategies for the novel configuration are studied.

A. Control Method of the Compensation currents

Based on the above analysis, two parts in the novel APF works independently to generate two current references separately. Therefore, the current control strategy based on the dual-hysteretic controller is given (as shown in Fig. 3(a)). By using the harmonic extraction algorithms, current reference i_C^* will be obtained. Two modified references will be obtained by using a high accuracy rectifier, each reference working as the current reference of each part.

This control strategy is advanced for the simplicity and reliability of the implementation. But two current controllers are needed, and the forward voltage drop of the rectifier introduces the zero-cross distortion into the control strategy, decreasing the compensation performance.

Actually, two drive signals could be derived with some logic circuit. In other words, desired current reference will be drawn with the same PWM drive signals as shown in Fig. 3(b). The final drive signals for part I and II are obtained after determining the polarity of the current reference i_C^*. Compensation current of each part is discontinuous and unipolar. This control strategy is based on a single-hysteretic controller (as shown in Fig. 4).

As Fig. 4 illustrates, a group of bipolar modulation signals Q are obtained by using a hysteretic controller. Meanwhile, the polarity of the current reference Q_0 is obtained by using a zero-crossing detector. Finally, drive signals Q_2 is obtained by taking "and" of Q_0 and Q; drive signals Q_1 is obtained by taking "or not" of Q_0 and Q.

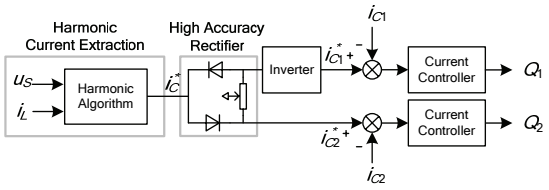

(a) Control scheme

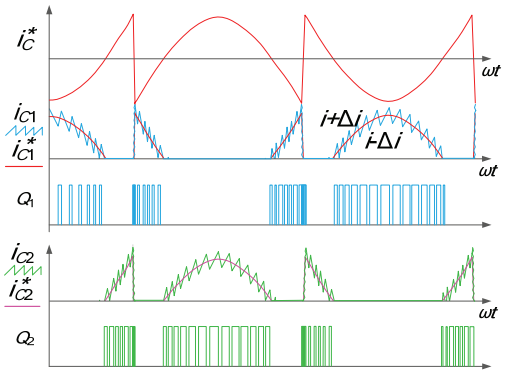

(b) Key operation waveforms

Figure 3. Control scheme and key operation waveforms of the dual-hysteretic controller based control strategy

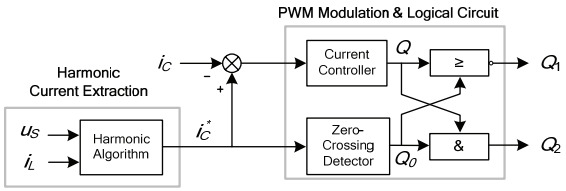

(a) Control scheme

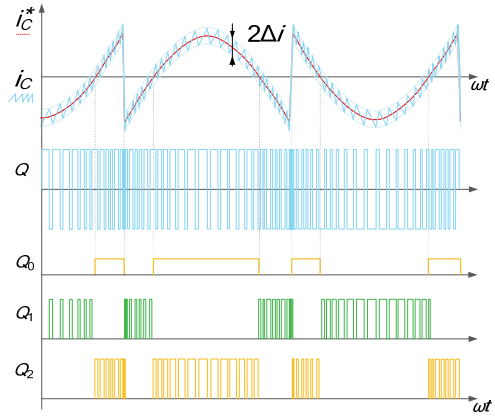

(b)Key operation waveforms

Figure 4. Control scheme and key operation waveforms of the single-hysteretic controller based control strategy

B. *DC-Link Voltage Control*

In order to keep the normal operation of the novel APF, dc-link voltage is need to be kept stable and balanced. Therefore, a practical voltage control strategy with high performance plays an important role to the compensation performance.

The dc-link voltage control consists of the overall voltage control and voltage balance control. The overall voltage control strategy has been studied and discussed in [5]. The error of dc-link voltage is sent into the voltage regulator, output is multiplied by the synchronous sinewave, to compose the final compensation current references. Essentially, overall voltage control loop introduces an active current into the compensation current to regulator the power exchanges between the power grid and APF, achieving the dc-link voltage stable. Synchronous sinewave is obtained by using a phase lock loop circuit, as shown in Fig. 5.

In order to balance the voltages of spit capacitors, the voltage error between the upper and lower capacitors is sent to the voltage balance regulator to derive a balance value. This

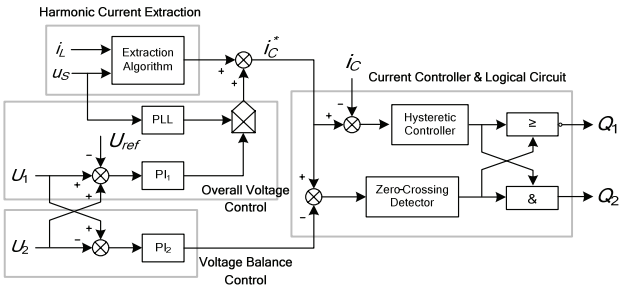

Figure 5. Overall control strategy containing voltage balance control for the proposed APF

value will be added to the original compensation current combined of the overall voltage controller's output, to derive the final current reference. Essentially, voltage balance control loop regulates power exchange's direction between the power grid and APF, achieving the dc-link voltage balanced.

IV. Simulation and Experimental Waveforms

In order to verify the feasibility of novel APF and validity of the voltage control strategy, simulations using the "Simulink" software package of the "Matlab" are taken. The system power capacity S is set as S = 3 kVA. Detailed parameters are given in Tab. I.

In the simulation, *p-q* theory is taken as the harmonic extraction algorithm. Fig. 6(a) and (b) illustrate the key simulation waveforms under inductive load and capacitive load. From up to bottom, waveforms of phase voltage u_{Sa}, load current i_{La}, source current i_{Sa} and compensation current i_{Ca} are given. After APF's action, source current becomes sinusoidal, keeps phase with phase voltage. In Fig. 6(a), peak value of

TABLE I. Parameters of 3 kVA Prototype

Parameter	Value
Phase voltage u_S/V	115
Lines frequency f_S/Hz	400
Power capacity S/kVA	3
Boost inductor L/μH	600
DC-link capacitor C/μF	1000
DC-link voltage U_{dc}/V	200

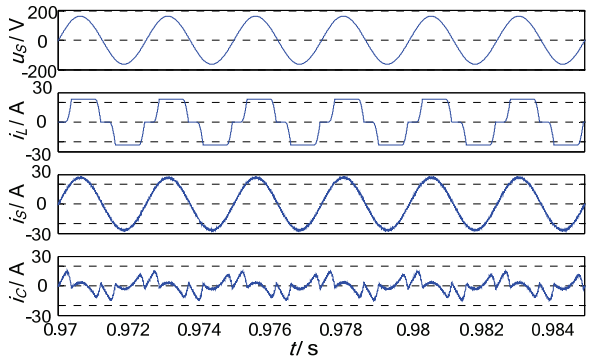

(a) Under inductive load

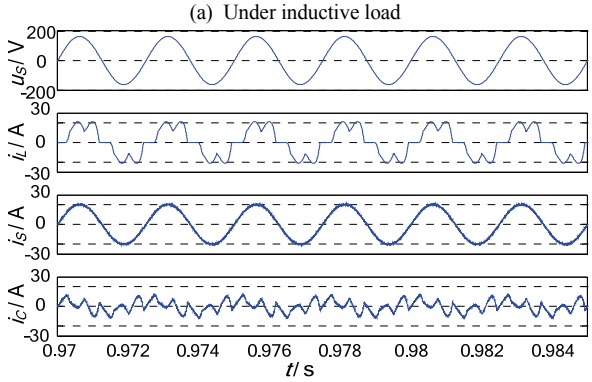

(b) Under capacitive load

Figure 6. Simulation waveforms under different load condition

compensation current reaches 16A, and the load's power capacity is as high as 6 kVA. THDs of the source currents are 1.90% and 24.32% with and without APF. In Fig. 6(b), peak value of compensation current reaches 12A, and the load's power capacity is as high as 4.5 kVA. THD of the source current decreases from 39.66% to 1.90% with APF's working. Good compensation performances are achieved for both current-source load and voltage-source load.

Fig. 7 illustrates the simulation waveforms of PWM drive signals, from up to bottom are Q_1, i_{C1}, i_{C2}, and Q_2. The currents i_{C1} and i_{C2} share the whole compensation current i_C, agreeing with the above analysis. In order to verify the validity of voltage balance control, a man-made unbalance test situation is made: one resistor is parallel connected with the upper capacitor, and no resistor connects with the lower capacitor.

Fig. 8 illustrates the simulation waveforms before and after

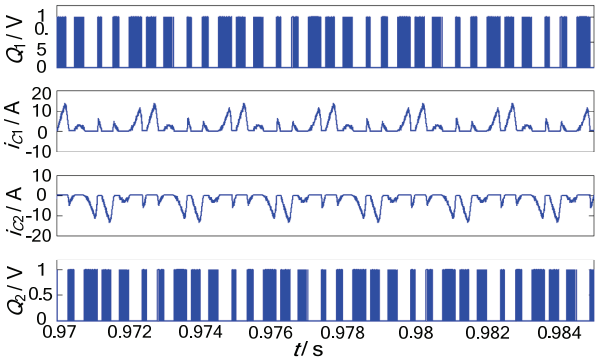

Figure 7. Simulation of the PWM drive signals and the compensation currents

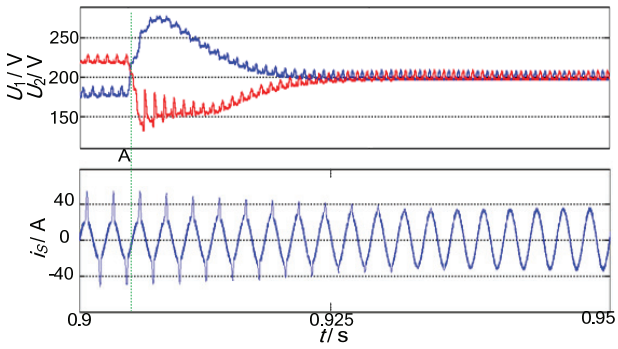

Figure 8. Simulation waveforms of voltage balance control test

enabling the voltage balance control. Before the voltage balance control works, U_1 and U_2 correspond to 180V and 220V, respectively. The source current does not get well compensated because of the reduced dc voltage U_1. After voltage balance controller's work, the dc link voltages get balanced, both 200V. The source current gets well compensated.

In order to verify the feasibility of the novel configuration, an aeronautical APF hardware prototype that has the same parameters with Tab. 1 is built in the laboratory. The power switch is SPW47N60C3, the diode is selected as DSEI30-06.

Fig. 9 illustrates the key experimental waveforms of novel

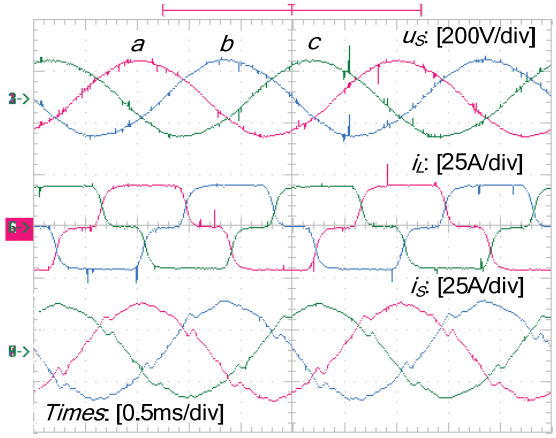

(a) Three-phase current waveforms

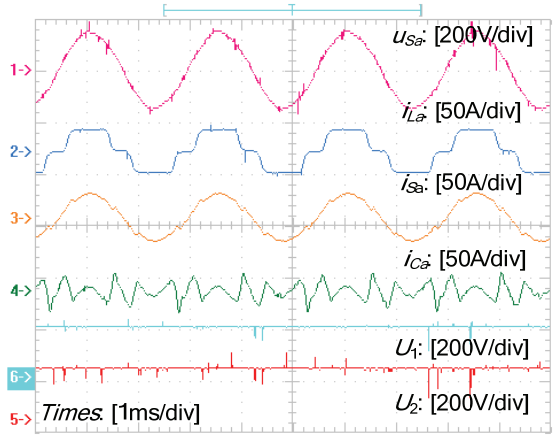

(b) Experimental waveforms of phase-*a*

Figure 9. Simulation waveforms under different load condition

APF under inductive load. Phase voltages, load currents and source currents of three phases are given in Fig. 9(a); phase voltage, load current, source current and compensation current of phase-*a* are given in Fig. 9(b). As Fig. 9 shows, harmonics in the aeronautical power system get well compensated; THDs of the three phase's source currents get reduced from 23.85%, 22.93%, and 23.48% to 4.996%, 4.394% and 4.832%. The dc-link voltages get stable to be around 200V, voltage control strategy achieving the good performance.

Fig. 10 illustrates the experimental waveforms of the inductor currents and PWM drive signals of phase-*a*. The negative -7V is helpful to turn off the Mosfet in a faster speed, and increase the robustness of the drive circuit.

Fig. 11 illustrates the key experimental waveforms of novel APF under capacitive load, phase voltage, load current, source current and compensation current of phase-*a* are given. The load power is as high as 4.5 kVA, and the peak value of the load current is 24A. As Fig. 11 shows, voltage-source nonlinear load in the aeronautical power system gets well compensated; THDs of the three phases' source currents get reduced to 7.492%, 6.933% and 6.732%. The source currents get improved, although have some notches in some points.

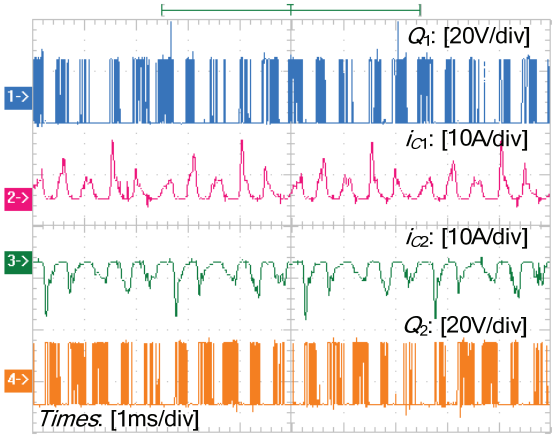

Figure 10. Experimental waveforms of the PWM drive signals and the compensation currents

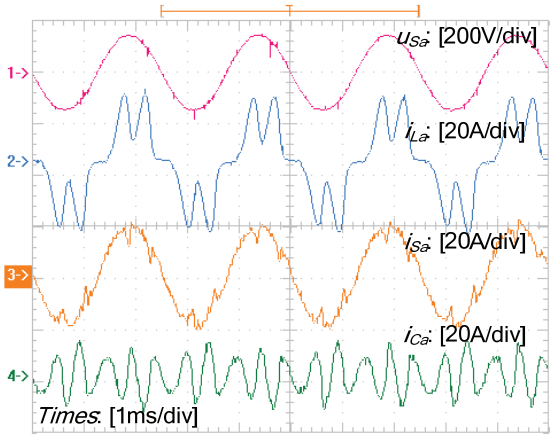

Figure 11. Experimental waveforms under capacitive load

V. Conclusion

In order to fulfill the high reliability of aeronautical application, a novel shunt APF with high reliability is proposed in this paper. The "shoot-through" phenomenon is eliminated by using the novel bridge leg composed of one power switch and one diode. Detailed operation principle and characteristic analysis are given as well, and the hysteretic current controller based control strategy and voltage balance control methods are studied. Finally, experimental waveforms from 6 kVA prototype confirm the feasibility of the novel APF and voltage balance control strategy. And the proposed topology is also suitable for other applications.

Acknowledgment

This work was supported by the National Nature Science of China under Award 51007037, Aeronautical Science Foundation of China under Award 2011ZC52041, and Foundation of Graduate Innovation Center in NUAA (kfjj20110205).

References

[1] J. A. Resero, J. A. Ortega, E. Aldabas, and L. Romeral, "Moving towards a more electric aircraft," IEEE Aerosp. Electron. Syst. Mag., vol. 22, no. 3, pp. 3-9, Mar. 2007.

[2] R. E. J. Quigley, "More electric aircraft," IEEE Applied Power Electronics Conference and Exposition, San Diego, CA, USA, pp. 906-911, Mar. 1993.

[3] A. Emadi and M. Ehsani, "Aircraft power systems: Technology, state of the art, and future trends," IEEE Aerosp. Electron. Syst. Mag., vol. 15, no. 1, pp. 28-32, Jan. 2000.

[4] E. H. J. Pallett, Aircraft Electrical Systems, 3rd ed. London, U.K.: Addison-Wesley, 1998.

[5] H. Akagi, "Active harmonic filters," Proc. IEEE, vol. 93, no. 12, pp. 2128–2141, Dec. 2005.

[6] H. Akagi, Y. Kannazawa, and A. Nabae, "Instantaneous reactive power compensators comprising switching devices without energy storage components" IEEE Trans. Ind. Appl., vol. IA-20, no. 3, pp. 625-630, May 1984.

[7] A. Eid, M. Abdel-Salam, H. El-Kishky and T. El-Mohandes, "Active power filters for harmonic cancellation in conventional and advanced aircraft electric power systems" Elect. Power Syst. Res., vol. 79, no. 1, pp. 80-88, Jan. 2009.

[8] A. Eid, M. Abdel-Salam, H. El-Kishky and T. El-Mohandes, "On Power Quality of Variable-Speed Constant-Frequency Aircraft Electric Power Systems" IEEE Trans. Power Delivery, vol. 25, no. 1, pp. 55-65, Jan. 2010.

[9] M. Odavic, P. Zanchetta and. M. Summer, "A Low Switching Frequency High Bandwidth Current Control for Active Shunt Power Filter in Aircrafts Power Networks," IEEE IECON 2007, pp. 1863-1868, Nov. 2007.

[10] E. Lavopa, M. Summer, P. Zanchetta, C. Ladisa and F. Cupertimo, "Real-time estimation of fundamental frequency and harmonics for active power filters applications in aircraft electrical systems", IEEE Transactions on Industrial Electronics, vol. 56, no. 8, pp. 2875-2884, August 2009.

[11] H. Hu, W. Shi, J. Xue, and Y.Xin, "A multi-resolution control strategy for DSP controlled 400Hz shunt active power filter in an aircrafts power system," in APEC 2010, pp. 1785-1791, Feb. 2010.

[12] Y. Wang and S. Shen, "Three-phase aeronautical active power filter based on space vector and one-cycle control," Journal of Beijing University of Aeronautics and Astronautics, vol. 33, no. 1, pp. 90-93, 109, Jan. 2007.